Neural and behavioral dynamics of encoding, production and synchronization with external rhythms in subcortical lesion patients

Antonio Criscuolo [1*], Michael Schwartze [1], Sylvie Nozaradan [2,3,4] & Sonja A. Kotz [1,5]

[1] Department of Neuropsychology & Psychopharmacology, Faculty of Psychology and Neuroscience, Maastricht University, 6200 MD, Maastricht, the Netherlands

[2] MARCS Institute for Brain, Behaviour and Development, Western Sydney University, Sydney, Australia

[3] International Laboratory for Brain, Music and Sound Research (BRAMS), Montreal, Canada

[4] School of Health and Behavioural Sciences, University of the Sunshine Coast, Queensland, Australia

[5] Department of Neuropsychology, Max Planck Institute for Human Cognitive and Brain Sciences, 04103, Leipzig, Germany

* Corresponding author

Email: a.criscuolo@maastrichtuniversity.nl

Abstract

Acting in and adapting to a dynamically changing environment necessitates precise encoding of the temporal unfolding of sensory events around us and to the *time* of our own (re-)actions to them.

Cerebellar (CE) and basal ganglia (BG) circuitries play fundamental and complementary roles in the timing of sensory events. While the CE seems to encode the precise timing of sensory events (*when* an event occurs), the BG engage in generating temporal predictions (*when* a next event occurs). However, their contributions are rarely investigated in combination, as it is generally difficult to record data from respective patient groups in parallel.

Here we investigated the contributions and causal roles of CE and BG in sensory and sensorimotor timing processing. Healthy controls and patients with lesions in either CE or BG listened to isochronous auditory sequences while their EEG was recorded and later performed a tapping synchronization task. We characterized intra- and inter-individual variabilities, as well as group differences, in delta-band phase-coherence, power fluctuations, and dynamics of acceleration, deviation and stability while tuning delta-band oscillations and tapping to the rhythm of the auditory sequence.

Combined behavioral and neurophysiological results confirm that patients displayed heterogeneity and altered capacity to synchronize ongoing neural activity and behavior with temporal regularities in the acoustic environment. These results confirm and differentiate the causal roles of the CE and BG in temporal processing as well as in the production and synchronization with temporally regular sound events.

1. Introduction

Time is a fundamental dimension of human cognition. Every decision, every action, every sensory stimulus around us happens in time and at multiple timescales. Our capacities to encode the precise *timing* of events and to *time* our (re-)actions to them are pivotal for acting and adapting to a continuously changing dynamic environment. However, the environment displays some gradient of *temporal regularity* (Greenfield, Honing, et al., 2021): there are various periodicities within the body (e.g., the heartbeat and respiration; Criscuolo et al., 2022) as well as in simple and complex sensory inputs (e.g., music, speech) and in behavior (e.g., interpersonal interactions in the animal and human world; Greenfield, Aihara, et al., 2021). These temporal regularities (or *rhythm*) can enable individuals to anticipate *when* an event starts and when the next sensory event occurs. In turn, temporal anticipation can benefit *adaptive* behavior: we can dance to music because we know *when* the next beat falls, and we can synchronize with others because their movement timing is predictable. Yet what determines our capacity to adapt behavior in time? Do we differ in the *if* and *how* we adapt and synchronize with auditory rhythms?

We have previously proposed (Criscuolo et al., 2023) that synchronization depends on two fundamental lower level capacities that form a 3-node framework: detect, produce, and synchronize ('DPS') with rhythms (Criscuolo et al., 2023). Encoding is a prerequisite to detect rhythms. Human (e.g., Schroeder & Lakatos, 2009) as well as nonhuman animals (e.g., Lakatos et al., 2008) can do so by aligning endogenous neural oscillatory activity at multiple timescales (Criscuolo et al., 2023; Lakatos et al., 2005) to temporal regularities in the sensory environment. Encoding and detecting regularities allow generating predictions about *when* next events occur, thus enabling the *dynamic attending* (Large & Jones, 1999) of event onsets. Temporal predictions materialize as anticipatory neural activity (Arnal, 2012; Fujioka et al., 2009, 2012, 2015; Ross et al., 2018; Snyder & Large, 2005), which supports the predictive alignment of neural oscillations to event onsets, fosters sensory processing (Lakatos et al., 2013) and further allows for production and synchronization of behavior in a predictive manner (Bartolo & Merchant, 2015; Gámez et al., 2018). Thus, "adaptation by anticipation" (Fraisse, 1963; p. 18) is a mechanism for optimizing behavior and operates across sensory modalities (Arnal & Giraud, 2012; Cravo et al., 2013; Friston, 2005; Morillon et al., 2016; Nobre et al., 2012).

Fundamental to predictive temporal processes is the engagement of an extended motor

system (Arnal, 2012; Fujioka et al., 2012, 2015), recruited to prepare and execute predictive and synchronized behavior. The cerebellum (CE) and the basal ganglia (BG) are structures in an extended subcortico-cortical brain network that plays a pivotal role in temporal processing (Schwartze & Kotz, 2013). The CE encodes the precise timing (*when* an event onsets) of sensory events in the subsecond range (Ivry et al., 1988; Ivry & Keele, 1989; Ivry & Schlerf, 2008) and thus allows estimating the duration of temporal intervals (Grube, Cooper, et al., 2010a; Grube, Lee, et al., 2010; Knolle et al., 2012, 2013; Teki, Grube, & Griffiths, 2011; Teki, Grube, Kumar, et al., 2011) by quantifying the time elapsed between event onsets. The BG support the generation of temporal predictions (*when* the *next* event occurs) and use relative timing to extract the beat (Grahn, 2009; Grahn & Brett, 2009a; Schwartze et al., 2011a; Teki, Grube, Kumar, et al., 2011). Consequently, patients with BG lesions are less sensitive to temporal regularity in auditory sequences, potentially resulting in a less efficient prediction of incoming sensory information in basic (Schwartze et al., 2015) as well as in complex (syncopated rhythms; Nozaradan et al., 2017) sequences. In contrast, CE lesions tend to not impact the capacity to generate temporal predictions (Schwartze et al., 2016b) but alter the encoding of event onsets in basic and complex sound sequences (Nozaradan et al., 2017), ultimately resulting in delayed and variable early event-related responses in the EEG (Schwartze & Kotz, 2021). Altered encoding of event onsets and single time intervals (Grube, Cooper, et al., 2010b) further affects the production of and synchronization with rhythms (Ivry & Keele, 1989; Ivry, Keele & Diener, 1988). CE lesion patients displayed larger heterogeneity in self-paced tapping and reduced capacities to synchronize their tapping to temporally regular sequences and tempo changes (Schwartze et al., 2016a). On the other hand, BG lesion patients showed intact synchronization when tapping to an external rhythm but also variable tapping behavior, indicating difficulties in coordinating and adjusting their tapping specifically to slower tempo changes (Schwartze et al., 2011b). Supporting prior lesion studies, these observations suggest intact single interval-based timing in the BG patients (Grube, Cooper, et al., 2010b; Teki, Grube, Kumar, et al., 2011), but impaired processing of temporal regularity (i.e., the hierarchical temporal structure of a sensory sequence, the beat) in music (Grahn & Brett, 2009b) and speech (Kotz & Schmidt-Kassow, 2015).

What underlies these dysfunctions? Can we relate difficulties in producing and synchronizing with external rhythms to specific neural dynamics? In other words, can the analysis of neural

oscillatory activity causally show in what way the cortico-subcortical timing network differentiates the processing of temporal regularities in perception and action?

We report results from two experiments involving healthy controls (HC) and patients with focal lesions in either the CE or BG. Via a behavioral and an EEG experiment, we assessed sensory and sensorimotor capacities to encode, produce, and synchronize neural activity and overt behavioral responses with temporal regularities in auditory sequences.

Participants listened to isochronous auditory sequences while EEG was recorded. We assessed *if*, *when*, and *how* their neural activity reflected the temporal regularity of auditory sequences. We expected CE patients to show increased variability in the temporal encoding of tone onsets, while we hypothesized BG patients to have difficulties in generating temporal predictions. To test these hypotheses, we developed an extensive analysis pipeline designed to quantify the *tuning* of delta-band neural oscillatory activity towards the stimulation frequency. In order, (i) time-frequency representation analyses allowed us to test for group differences in the power of neural activity in the delta-band. Next, (ii) instantaneous frequency (IF) analyses were employed to test whether delta-band neural activity would tune to the stimulation frequency (*Sf*) of the auditory sequence (1.5Hz). Third, (iii) acceleration analyses quantified the dynamics of oscillatory activity over time, once transformed into IF. (iv) Acc values were further used to compute a metric of Stability (inversely proportional to the sum of dynamic changes in the Acc over time). Similarly, (v) from IF we derived a metric of Deviation, which quantifies the standard deviation of IF from the *Sf* over time. Lastly, (vi) we complemented these metrics with a measure of Shannon entropy (E) of Pow, IF and Acc. Overall, these methods allowed to test the hypotheses that CE lesions should causally impact the ability to encode the precise timing of event onsets (variability in the IF, low ITPC and Dev), while BG lesions should causally impact the capacities to process temporal regularities and generate temporal predictions (low delta power, heterogenous IF and Acc, resulting in low S).

In the behavioral experiment, we expected the patient groups to display difficulties in producing stable finger-tapping and to synchronize to regular auditory sequences presented at three different tempi. We hypothesized that CE patients would have difficulties in the precise encoding of event onsets and synchronizing behavior, especially with faster tempi, while BG patients were expected to have more difficulties producing and synchronizing with slower rhythms. To test these hypotheses, we conducted comprehensive within- and between-group analyses of

individual dynamics of tapping, quantifying tapping rates, acceleration, entropy, and stability of the performance over time.

2. Materials & Methods

2.1. Participants

Thirty-three participants took part in the study and signed written informed consent in accordance with the guidelines of the ethics committee of the University of Leipzig and the declaration of Helsinki. Participants comprised two patient groups and one age- and gender-matched control group: 11 patients with focal lesions in the basal ganglia (BG; mean age 50.9, range = 30-64 years; 5 males), 11 patients with focal lesions in the cerebellum (CE; mean age 52.6, range = 37-64 years; 5 males), and 11 healthy controls (HC; mean age 52.1, range = 28-63 years; 5 males). Patients' demographics and lesion information are provided in Tab. 1, their anatomical MRI is provided in Fig. 1, and the results of their neuropsychological and cognitive assessment are provided in Suppl. Tab. 1.

The HC group was recruited via a database at the Max Planck Institute for Human Cognitive and Brain Sciences (Leipzig, Germany). All participants were right-handed and matched for years of education. None of the participants were professional musicians, and they reported no history of hearing or psychiatric disorders. All participants received monetary compensation for taking part in the study. Further information on the participants and lesions characteristics can be found in Nozaradan et al., (2017).

CE	*Age*	*Location*	*Additional locations*	*Etiology*	*Volume in cc*	*X*	*Y*	*Z*
	64	posterior cerebellar lobule	none	PICA infarction	7,1	89	37	26
	30	posterior cerebellar lobule	superior frontal gyrus, corpus callosum	ICH and AVM	48	77	38	35
	49	posterior cerebellar lobule, tonsil, vermis	none	PICA infarction	14,5	57	40	24
	53	anterior and medial cerebellar lobule, tonsil	none	PICA infarction	7,9	62	41	24
	39	anterior and posterior cerebellar lobule	none	cyst extripation	2,4	88	52	15
	62	posterior cerebellar lobule	thalamus	PICA infarction	9	111	69	37
	62	posterior cerebellar lobule	telencephalic white matter	PICA infarction	3,1	57	58	55
	59	posterior cerebellar lobule, tonsil	none	PICA infarction	3,6	110	38	30
	63	posterior cerebellar lobule	telencephalic white matter	PICA infarction	5,7	104	61	46
	37	vermis, deep cerebellar nuclei, peduncle	none	tumor postoperatively	8,8	84	49	37
	42	posterior cerebellar lobule	none	PICA infarction	0,3	121	48	27
BG								
	41	putamen, pallidum, caudate body, IC	corona radiata	MCA infarction	23,4	56	113	76
	59	putamen, pallidum, caudate head and body, IC	corona radiata	ICH	18,3	53	119	76
	52	putamen	none	ICH	2,8	104	99	74
	61	claustrum, putamen, pallidum, caudate body, EC, IC	corona radiata, thalamus	ICH	8,8	51	98	77
	37	putamen, caudate body, IC	none	MCA infarction	0,8	55	97	88
	50	putamen, caudate body, IC	corona radiata, corpus callosum	MCA infarction	6,7	54	110	81
	60	putamen	none	MCA infarction	0,5	47	102	64
	55	putamen, pallidum, caudate body	none	MCA infraction	3,0	102	101	77
	51	claustrum, putamen, EC	insula	ICH	14,8	106	102	78
	64	putamen, pallidum, caudate body, IC	none	MCA infaction	6,1	98	116	80
	49	putamen, caudate body	thalamus	MCA infarction	6,3	93	103	82

Table 1 – Individual patient history.

In order, from left to right, age, lesion location, secondary lesion location, lesion etiology, volume of the lesion in cc, and lesion coordinates (as provided by MRIcron). Top for cerebellar (CE) patients, and bottom for basal ganglia (BG) patients. Abbreviations: PICA = posterior cerebellar artery, ICH = intracerebral/-cerebellar hemorrhage, AVM = arteriovenous malformation, IC = internal capsule, EC = external capsule, MCA = Middle cerebral artery. The highlighted rows indicate patients for which both EEG and tapping data were used.

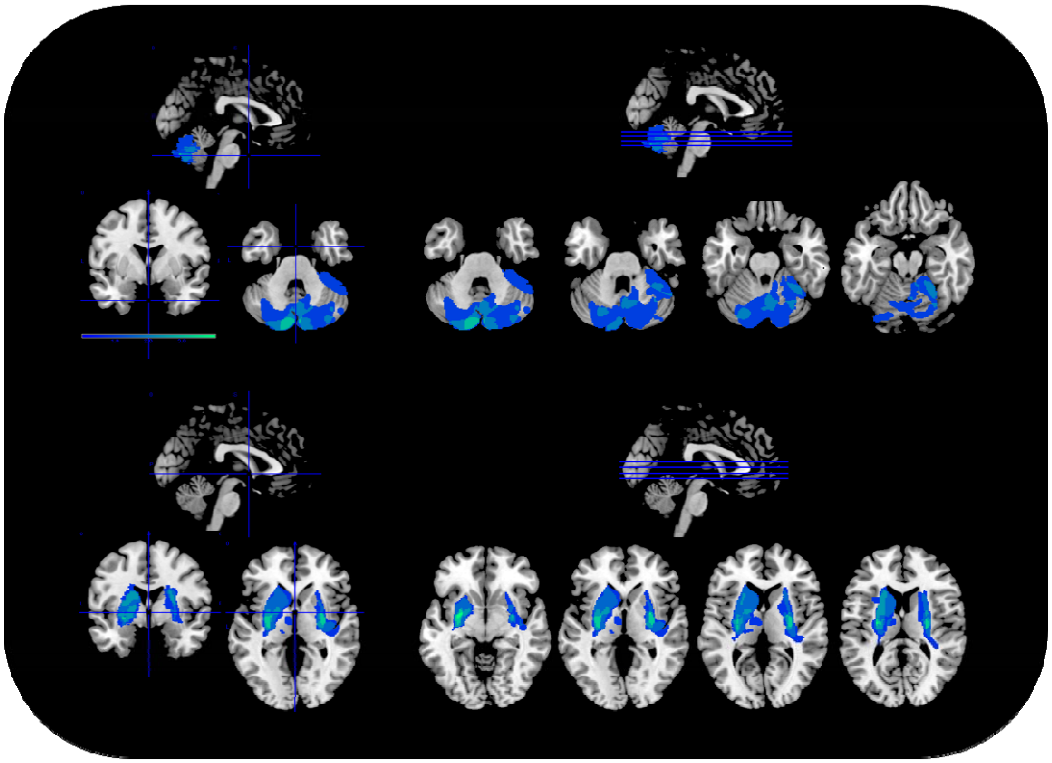

Figure 1 – Brain lesion delineation and overlap.

The figure provides the brain lesion delineation on a template anatomical MRI for basal ganglia (BG; top) and cerebellar (CE; bottom) patients. The figures were obtained by using MRIcron (http://www.mccauslandcenter.sc.edu/mricro/mricron/), and display the lesion overlap color-coded in shades of blue (blue = minimal overlap; light blue high overlap; values range from 0 to 5).

2.2.EEG experiment: design and procedure

Participants listened to 96 sequences comprising 13-to-16 tones in a recording session of approximately 25min. Each sequence contained frequent standard tones (STD; F0 = 400Hz, duration = 50ms, ramp up and down = 10ms, amplitude = 70dB SPL) and one or two amplitude-attenuated deviant tones (DEV; amplitude 66dB). The inter-onset-interval between successive tones was 650ms, resulting in a stimulation frequency (*Sf*) of 1.54Hz, and a total sequence duration of 8.45-10.4s (13 to 16 tones * 650ms; Fig. 2A).

Participants were seated in a dimly lit soundproof chamber facing a computer screen. Every trial started with a fixation cross (500ms), followed by the presentation of an auditory sequence. The cross displayed on the screen served to prevent excessive eye movements during the presentation of the tone sequences. At the end of each sequence, participants were prompted to press a response button to indicate whether they had heard one or two softer tones. After this response, there was an inter-trial interval of 2000ms. A session was divided into two blocks of

approximately 10 minutes each, with a short pause in between.

2.2.1. EEG recording

The EEG was recorded by means of 59 Ag/AgCl scalp electrodes positioned according to the International 10-10 system with the ground placed on the sternum. Four additional vertical and horizontal electrodes monitored eye movements and were positioned on the outer canthus of each eye, and on the inferior and superior areas of the left orbit. The signals were amplified, low-pass filtered at 512Hz, digitized using a sampling rate of 1024Hz (64-channel high-speed amplifier, Biosemi, the Netherlands). Electrode impedances were kept below 5kΩ and the left mastoid served as online reference. Data were referenced to an average reference offline.

2.2.2. Data Analysis

EEG Preprocessing

EEG data were analyzed in MATLAB with a combination of custom scripts and functions and the FieldTrip toolbox (Oostenveld et al., 2011). Data were band-pass filtered with a 4th order Butterworth filter in the frequency range of 0.1-50Hz (*ft_preprocessing*). Eye-blinks and other artifacts were identified using independent component analysis. This semi-automated routine is composed of two steps: in the first iteration, '*fastICA'* (implemented in FieldTrip) was applied to decompose the original EEG signal into independent components (N= number of EEG channels - 1). Components with a strong correlation (>.4) with the EOG time-courses were automatically identified and removed with '*ft_rejectcomponent*' before reconstructing the EEG time-course. In a second step, '*fastICA'* was used again, now with a dimensionality reduction to 20 components. These components were visually inspected via 'ft_*rejectvisual'* and marked as 'outliers' if their max values and z-scores were far from the distribution of other components. The 20 components were further visually inspected by plotting their topographies and time-series, and a second selection of 'outliers' was made. Taking into consideration the two visual inspections, we made a final decision on which components to remove. On average, 2 components were removed ('*ft_rejectcomponent*') before reconstructing the EEG time-series. In the next preprocessing step, artifact subspace reconstruction was performed as implemented in the '*pop_clean_rawdata*' function in EEGlab, and with the 'BurstCriterion' parameter set to 20 (as recommended in the online EEGlab tutorials; all other parameters were set to 'off'). To further ensure the removal of

potentially noisy channels and time-points, we implemented an automatic channel rejection and an artifact suppression procedure. To this end, the median variance across channels was calculated (excluding EOG channels), and channels exceeding 2.5*median variance were defined as 'outliers' and removed. Similarly, the artifact suppression procedure (see Criscuolo et al., 2023) interpolated noisy (>2.5*absolute median) time-windows on a channel-by-channel basis. Lastly, data were low pass filtered at 40Hz via '*ft_preprocessing*', segmented to each auditory sequence (starting 4s before the first tone onset and ending 4s after the last tone onset), and downsampled to 100Hz.

Fast-Fourier Transform and Inter-Trial Phase coherence

Fast-Fourier transform (FFT) analyses were conducted to test whether healthy participants and patients encoded temporal regularities in the auditory sequences. FFT analyses were performed at the single-participant, -channel and -trial level on 8s-long segments starting from the onset of the first tone in the auditory sequence and including a total of 12 tones. The resulting frequency resolution was .125Hz (1/8s = .125Hz). As in prior work (Criscuolo et al., 2023), a fronto-central channel (FC) cluster was used, encompassing the sensor-level correspondents of prefrontal, pre-, para-, and post-central regions highlighted in (Fujioka et al., 2012; Fujioka et al., 2015). The cluster included 14 channels: 'AFz', 'AF3', 'AF4', 'F3', 'F4', 'F5', 'F6', 'FCz', 'FC3', 'FC4', 'FC5', 'FC6', 'C3', 'C4'. Data from this FC cluster were not averaged at this stage. Next, the complex part of the Fourier spectrum was used to calculate inter-trial phase coherence (ITPC; Fig. 2B left). ITPC was obtained by dividing the Fourier coefficients by their absolute values (thus, normalizing the values to be on the unit circle), averaging, and finally taking the absolute value of the complex mean (for further documentation see https://www.fieldtriptoolbox.org/faq/itc/). For illustration purposes, the ITPC plots in Fig. 2B are restricted to 1-4Hz.

As the stimulation frequency of the auditory sequences was 1.5Hz, we restricted single-participant and -channel ITPC analyses at 1.5Hz only, and disregarded any other frequencies including (sub)harmonics of the stimulation frequency. Finally, single-participant and -channel data were pooled per group and visualized as violin plots in Fig. 2B (right). Group differences were statistically assessed by means of a 1-way ANOVA with a group factor (*anova1* built-in in MATLAB), followed by post-hoc simple tests corrected for multiple comparisons via Tukey-Davis correction (*multcompare* built-in in MATLAB) in case of a significant (p <.05) main

effect (Suppl. Tab. 2). Simple effects with a *p*-value below an alpha-corrected .05 were considered statistically significant.

Analyses of oscillatory dynamics

We employed several methods to analyze neural oscillatory activity pre-, during, and post-stimulation (listening periods). Details and parameters for each of the methods are provided in the respective sections below.

Time-frequency transform

After preprocessing, single-trial EEG data underwent time-frequency transformation (‘*ft_freqanalysis’*) by means of a wavelet-transform (Cohen, 2014). The bandwidth of interest was centered around the stimulation frequency (+/- 1Hz, i.e., .54 - 2.54Hz, thus obtaining a 1.54Hz center frequency), using a frequency resolution of .2Hz. The number of fitted cycles was set to 3. The single-trial approach results in ‘induced’ (as compared to ‘evoked’) responses. No averaging over channels, trials, or participants was performed at this stage. The resultant time-frequency transformed data was labeled as ‘Pow’.

Instantaneous frequency

After preprocessing, single-trial EEG data were bandpass-filtered with a 4th order Butterworth filter centered around the stimulation frequency (plus and minus 1Hz, .54 - 2.54Hz, obtaining a 1.54Hz center frequency; *ft_preprocessing*) and Hilbert-transformed to extract the analytic signal. Next, the instantaneous frequency (IF) at each time point (t), and for each channel, trial, and participant, was calculated with the following formula:

$$IF(t) = \frac{FS}{2\pi}\,\omega(t) = \frac{FS}{2\pi}\,\frac{d\theta(t)}{dt}$$

Where ω(t) is the derivative of the unwrapped phase (θ) at each time point (t), given the time-steps (dt) and FS is the sampling frequency.

Acceleration

Once calculated the single-participant, -trial, and channel-level IF, acceleration (Acc) was calculated as the first derivative of IF (or as the second derivative of the Hilbert-transformed

signal). Thus, we employed the following formula:

$$Acc(t) = \frac{d\ IF(t)}{dt}$$

Stability

Once the single-participant, -trial, and channel-level Acc was obtained, Stability (S) was calculated as the inverse of the sum of absolute changes in Acceleration. Thus, we employed the following formula:

$$S(X) = \frac{1}{\sum_1^N |Acc|}$$

Deviation

Once the single-participant, -trial, and channel-level IF was obtained, we quantified the deviation (D) from the stimulation frequency. D was calculated as the square-root of the mean squared difference between the IF and the stimulation frequency (Sf):

$$D(X) = \sqrt{\frac{1}{N}\sum_1^N\left(\left(IF\ - Sf\right)^2\right)}$$

Mean and Entropy Pre-, During, and Post-sequence

For each participant, trial, and channel, we calculated the mean and entropy of Pow, IF and Acc in three time-windows of interest: pre-sequence ('Pre'; -4 to 0s), during the sequence ('Dur'; 0 to 8.45s), and post-sequence ('Post'; 8.45 to 12.45s). Shannon entropy (E) was calculated with the following formula:

$$E(X) = -\sum_{x\ \epsilon X} p(x)\ \log\ p(x)$$

Where Σ denotes the sum over the variable's possible values and p is the probability of each value (x) in the time-series (X).

Latency

For each participant, trial, and channel, we estimated how long it took for the IF to tune to the *Sf* (1.5Hz). The search was performed within the first 8s of listening (0-8s) of each trial, and by using a narrow frequency criterion (*Sf* ± .2Hz).

Statistical comparisons

Group differences were statistically assessed for each of the above-mentioned metrics by means

of a 1-way ANOVA with a group factor (*anova1* built-in in MATLAB), followed by post-hoc simple tests corrected for multiple comparisons (Tukey-Davis correction) (*multcompare* built-in into MATLAB) in case of a significant (p <.05) main effect. Simple effects with a p-value below an alpha-corrected .05 were considered statistically significant and are reported as horizontal black lines on top of Fig. 3B. The ANOVA tables and simple tests are provided in the Supplementary materials (Tab. 3-10).

2.3. Tapping experiment

The same participants also performed the tapping experiment. However, not all could complete the tapping task. We therefore present data from 7 matched participants per group. The participants who took part in both experiments are highlighted in Tab. 1.

For the tapping experiment, participants listened to the same auditory stimuli as the ones employed in Nozaradan et al., 2017. They were composed of 12 intervals of 200ms and comprised pure tones (1000Hz) with 10ms rise and fall times and silent intervals (Fig. 4A). Such shortest inter-onset intervals (IOI) define a basic stimulation frequency (*Sf*) of 5Hz. The sequences were further presented at two more tempi: double ('x2', resulting in a 10Hz *Sf*), and quadruple ('x4', resulting in a 20Hz *Sf*) base tempo. Each sequence (12 intervals) was looped continuously for 33s, resulting in a total duration of ~5.5min.

Participants were asked to tap with the index finger in time with the perceived beat in an auditory stream and were instructed to start tapping as soon as they perceived the beat. Differently from the EEG experiment, this task required participants to process the rhythm, extract the salient periodicity from the acoustic sequence and coordinate their movements to it.

Tapping was performed on a response pad while the forearm and elbow were fixed on an armrest cushion to avoid excessive movements. Taps did not trigger any sound, and the latency of each finger tap (i.e. the time of contact of the finger onto the pad) was registered with millisecond accuracy and recorded in Presentation (NBS, Berkeley, USA).

2.3.1. Tapping data analysis

Based on tapping time data, we obtained the inter-tap-interval (ITI) as the difference between successive tap onsets. Next, we calculated the Shannon entropy and the Stability in ITI with the same formulas as described above. Lastly, we obtained the tapping frequency (Freq) as the

inverse of the ITI (1/ITI).

Individual data were pooled for each group (Fig. 4B-C). We then performed two main statistical comparisons: within-group and between-group differences. For the latter, between group differences were assessed for the basic tempo, 'x2' tempo, and 'x4' tempo. In Fig. 4C, we display from left to right the group data for the ITI, Freq, and Stability, color coded per group. For the within group assessment, the same variables were displayed per group, assessing differences across tempi (color coded per tempo; basic, 'x2' and 'x4').

Between and within group differences were statistically assessed only for the ITI by means of a 1-way ANOVA with a group factor (*anova1* built-in in MATLAB), followed by post-hoc simple tests corrected for multiple comparisons by Tukey-Davis correction (*multcompare* built-in in MATLAB) in case of a significant (p <.05) main effect. Simple effects with a p value below an alpha-corrected .05 were considered statistically significant and are reported as horizontal black lines on top of Fig. 4. The ANOVA tables and the simple tests are provided in the Supplementary materials (Tab 11-16). No statistical comparisons were performed on the other metrics due to low statistical power (one value per subject, resulting in 7 values per group).

2.4. Link between Tapping – EEG data

Despite the low number of participants, exploratory analyses aimed to assess a possible link between tapping and EEG data by means of Pearson correlation. We correlated the EEG metrics of ITPC, Pow E, IF E, Acc E, Stability, Deviation, and Latency with tapping metrics of Entropy and Stability. Correlations were assessed at the single-participant level, and independently for the three tempi. Finally, the results were visualized by means of circular graphs in Fig. 5 (rho values are provided in Suppl. Fig. 27).

2.5. Data and code Availability

The analysis code in use will be stored in an open repository.

3. Results

In this study, we investigated how sensory and sensorimotor capacities are shaped by temporal regularities in auditory sequences comparing HC, CE, and BG patients. Hence, we report results

from two experiments: first, participants listened to isochronous auditory sequences while EEG was recorded continuously (Fig. 2). Next, the same individuals performed a tapping task, in which they synchronized their tapping to regular auditory sequences presented at three different tempi (Fig. 4).

3.1. EEG experiment

In this experiment, we adopted two methodological approaches. First, we employed Inter-Trial-Phase Coherence (ITPC) analyses to investigate *if* and *how* HC, BG and CE participants encoded temporal regularity in auditory sequences. Second, analyses of neural oscillatory dynamics assessed *if*, *when*, and *how* participants' neural activity *tuned in* and *out* of temporal regularity in acoustic sequences. Details for each methodological approach can be found in the respective methods section above. Results for each method are discussed below, in two separate paragraphs.

3.1.1. Inter-Trial Phase coherence (ITPC)

While participants listened to isochronous auditory sequences presented at a *Sf* of 1.5Hz (Fig. 2A), their neural activity encoded the temporal regularity, as shown by the coherence peaks at 1.5Hz in the ITPC spectrum (Fig. 2B). A distinct peak at 1.5Hz was present in the ITPC spectrum for all groups (Fig. 2B, left). However, statistical analyses revealed a significant group difference (Fig. 2B, right): HC (dark blue) showed stronger coherence at the *Sf* than both CE and BG groups (lighter shades of blue). The one-way ANOVA revealed a significant group effect ($p < .001$; Supp. Tab. 2), and post-hoc simple t-tests revealed higher coherence in HC than in both CE and BG groups, but no significant difference between CE and BG (Suppl. Tab. 2; corrected for multiple comparisons).

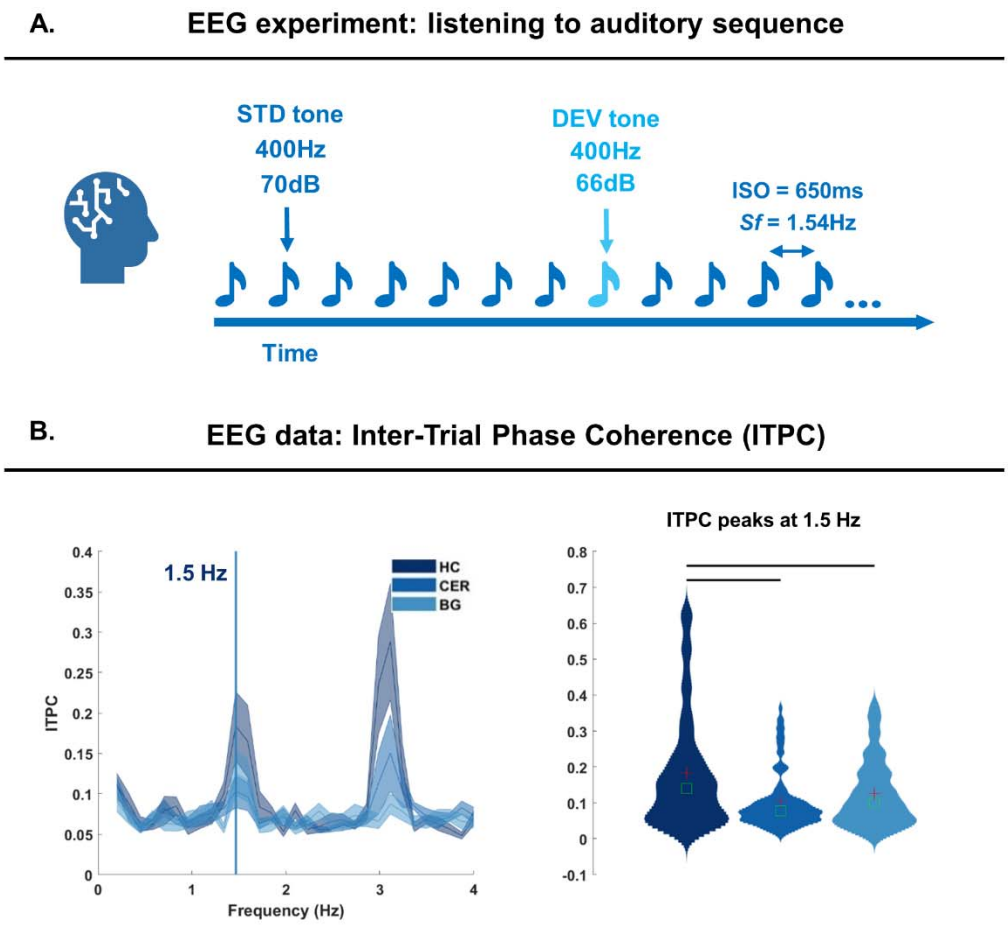

Figure 2 – Experimental design of the EEG study, and Inter-Trial Phase Coherence analyses.

A: experimental design: participants listened to 96 isochronous auditory sequences presented at a fixed Stimulation frequency (Sf) of 1.54 Hz (inter-stimulus onset (ISO) of 650ms). The sequences included frequent standard (STD; pitch 440Hz, loudness 85dB) and infrequent amplitude deviant (DEV) tone (amplitude 66dB). B: Inter-Trial Phase Coherence (ITPC) analyses. The ITPC plot features frequency in Hz on the x-axis and the ITPC values on the y-axis. Healthy controls (HC), cerebellar (CE) and basal ganglia (BG) patients' data are provided in shades of blue (from dark to light blue). The vertical blue line signals the ITPC peak at 1.5Hz. These peaks were extracted and plotted on the right, via means of distribution plots. Here, statistical comparisons assessed group differences in ITPC values at the stimulation frequency (1.5Hz). The black horizontal lines report significant differences between the groups, after correction for multiple comparisons.

3.1.2. Neural oscillatory dynamics of rhythm processing

Single-participant estimations

Each of the metrics mentioned above were estimated at the single-participant and –trial level, as illustrated in Fig. 3A: the time-course of Hilbert-transformed data, IF and Acc (solid line = mean over channels; shaded bars report the standard error (SE) over channels). The dashed pink line on the IF plot, reports the *Sf*. On the right side, the distribution of IF and Acc in the 'Pre-', 'Post-'

and 'Dur-'(ing) the listening periods (color-coded in shades of blues), and pooling across the FC channel cluster. The time-series of IF and Acc were further used to estimate D, the deviation from the *Sf*, and S, the stability of the neural signal. Finally, we obtained the Latency (not visualized here), the first crossing point of IF through the horizontal *Sf* line. The single-participant and -trial figures (33 participants x 96 sequences) can be provided upon reasonable request.

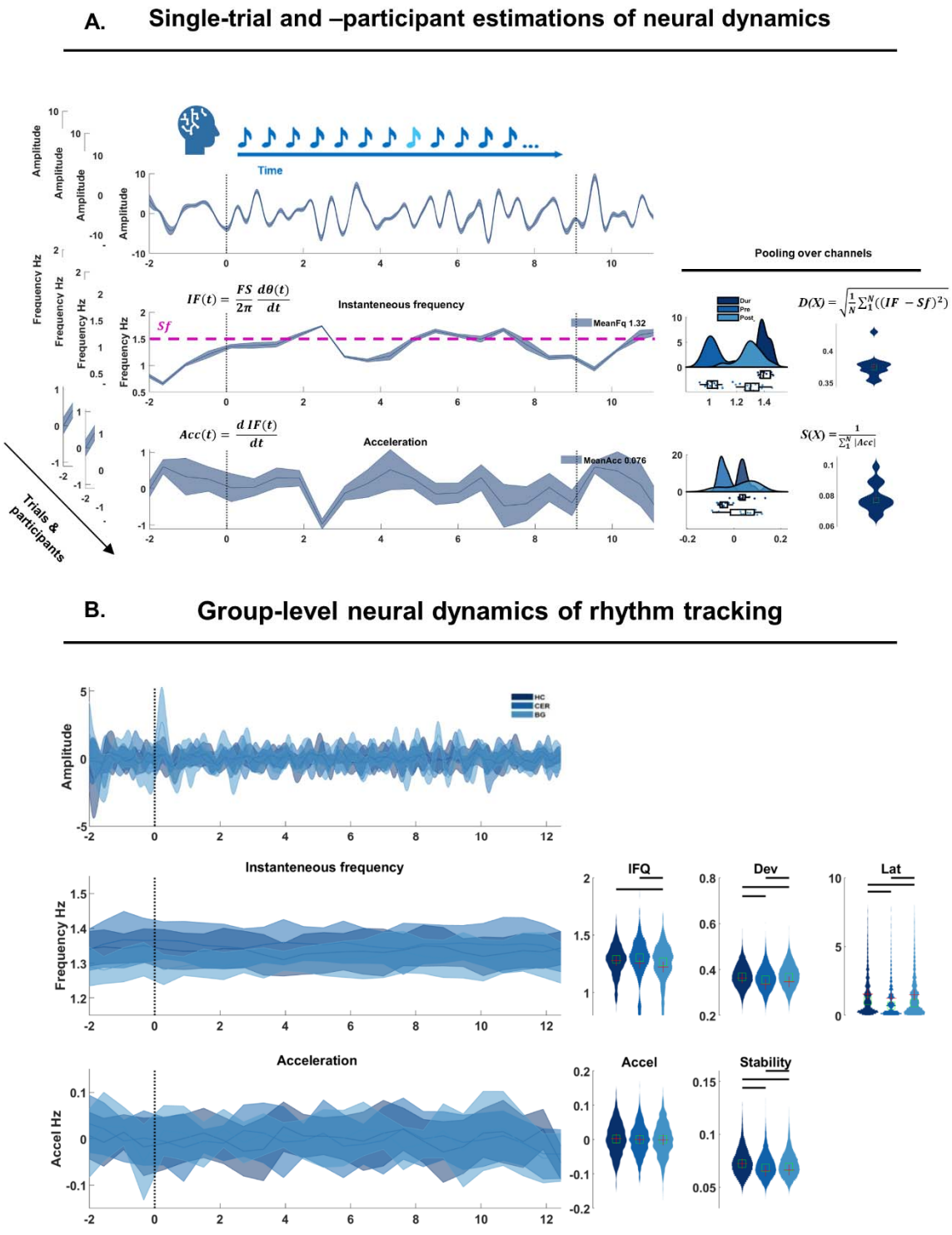

Figure 3 – Analyses on neural dynamics of rhythm processing.

A: We estimated, at the single-participant and -trial levels, the instantaneous frequency (IF) and Acceleration (Acc; time-courses on the left side). The pink dashed line on top of the IF indicates the stimulation frequency (Sf). The distribution plots on the right side are obtained by pooling data points over channels and averaging over time. IF and Acc were also used to calculate metrics

of Deviation (D) and Stability (S). The violin plots on the right side show the resultant D and S over time, and pooling over channels. B: mirroring the layout of A, the group-level data (color-coded in shades of blue) reporting on the left the time-courses of neural oscillations in the delta frequency band (top), the estimated IF (middle) and Acc (bottom). On the right side of the IF time-courses, violin plots of the IF pooling over trials and participants and averaging across the FC cluster of interest. Next to it, the estimated Dev values, and the Latency. Next to the time-courses of the Acc, violin plots of the Acc pooling over trials and participants and averaging across the FC cluster of interest. Next to it, the estimated S values. The thick black horizontal lines on top of the violin plots report significant group differences ($p < .001$, corrected for multiple comparisons).

Group visualization

Individual data were then pooled into 3 groups: HC, CE, and BG patients. The group-level data is provided in Fig. 3B and mirrors the layout of Fig. 3A.

On the right side, the violin plots show (in order) the IF and Acc, obtained by averaging data during the listening window (0-8s) and across channels, and by pooling single-participant and -trial data. Next to it, are the distributions of Dev, S and latency obtained by averaging over channels, and pooling over participants and trials. Note that for readability, Fig. 3 focuses on the listening period ('Dur') only, avoiding visualizations of Pre- and Post-listening periods. Similarly, Fig. 3 excludes data from Entropy analyses. Statistical comparisons are provided in Suppl. Tables, while additional figures are stored in a personal drive, and can be provided upon reasonable request by the authors.

HC's Pow and IF was like that of CE patients, but significantly different from BG patients (Suppl. Tab. 2,4). HC's Dev and Lat were higher than both patients' groups (Suppl. Tab. 9,10). There were no significant differences in Acc, but HC had a significantly higher S as compared to the two groups (Suppl. Tab. 8).

In contrast, CE patients showed the lowest Dev and Lat (Suppl. Tab. 9,10), comparable Acc (Suppl. Tab. 6) and the lowest S (Suppl. Tab. 8).

Finally, BG patients' neural activity showed higher power (Suppl. Tab. 2) and lower IF (Suppl. Tab. 4) during listening as compared to both HC and CE. Their Dev, Lat, and S was higher than CE but lower than HC (Suppl. Tab. 8,9,10).

3.2. Tapping experiment

Participants listened to auditory sequences at 3 rates (basic tempo, 'x2' and 'x4' tempo; Fig. 4) and were asked to synchronize their tapping to the perceived beat and try to keep tapping at a comfortable rate. Within- and between-group comparisons assessed tapping behavior and variability over time. Starting from the within group analyses (Fig. 4B), HC's ITI followed an

inverse U-shape, whereby ITI increased from the basic to the ‘x2’ tempo and decreased for the highest rate (‘x4’ tempo; Suppl. Tab. 15). The ‘x4’ showed the shortest ITI as compared to the other two tempi, thus resulting in the highest tapping frequency. Tapping stability tended to increase linearly over the tapping rates.

CE patients’ tapping behavior was comparable to the one found for HCs: their ITI showed an inverse U-shape, whereby the ITI was significantly longer in the ‘x2’ tempo as compared to the basic and ‘x4’ tempi, and the latter had the shortest ITI (Suppl. Tab. 16). Thus, the resulting tapping frequency increased across rates, and so did the tapping stability.

Finally, the BG patients showed a negative linear relationship between tapping speeds and ITI, whereby the ITI were longest for the basic tempo and shortest for the ‘x4’ (Suppl. Tab. 17). Thus, their resulting tapping frequency followed a U-shape across tempi, and their stability increased with ‘x4’ tempo.

Moving to between-group differences (Fig. 4C), BG patients’ ITI were largely variable across individuals, as revealed by both within- and between-group analyses. In fact, some of the patients tapped at high frequencies, and others at a slow frequency, especially at the basic tempo. However, the average ITI at basic tempo was significantly longer than for the other two groups, who did not significantly differ from each other (Suppl. Tab. 12). CE patients showed longer ITI and high stability at ‘x2’ (Suppl. Tab. 13), and higher ITI at ‘x4’ tempo (Suppl. Tab. 14) as compared to the other two groups. BG had the lowest ITI at ‘x2’ tempo, and the lowest stability at ‘x4’ tempo. HC had the lowest ITI and the highest stability at ‘x4’ tempo.

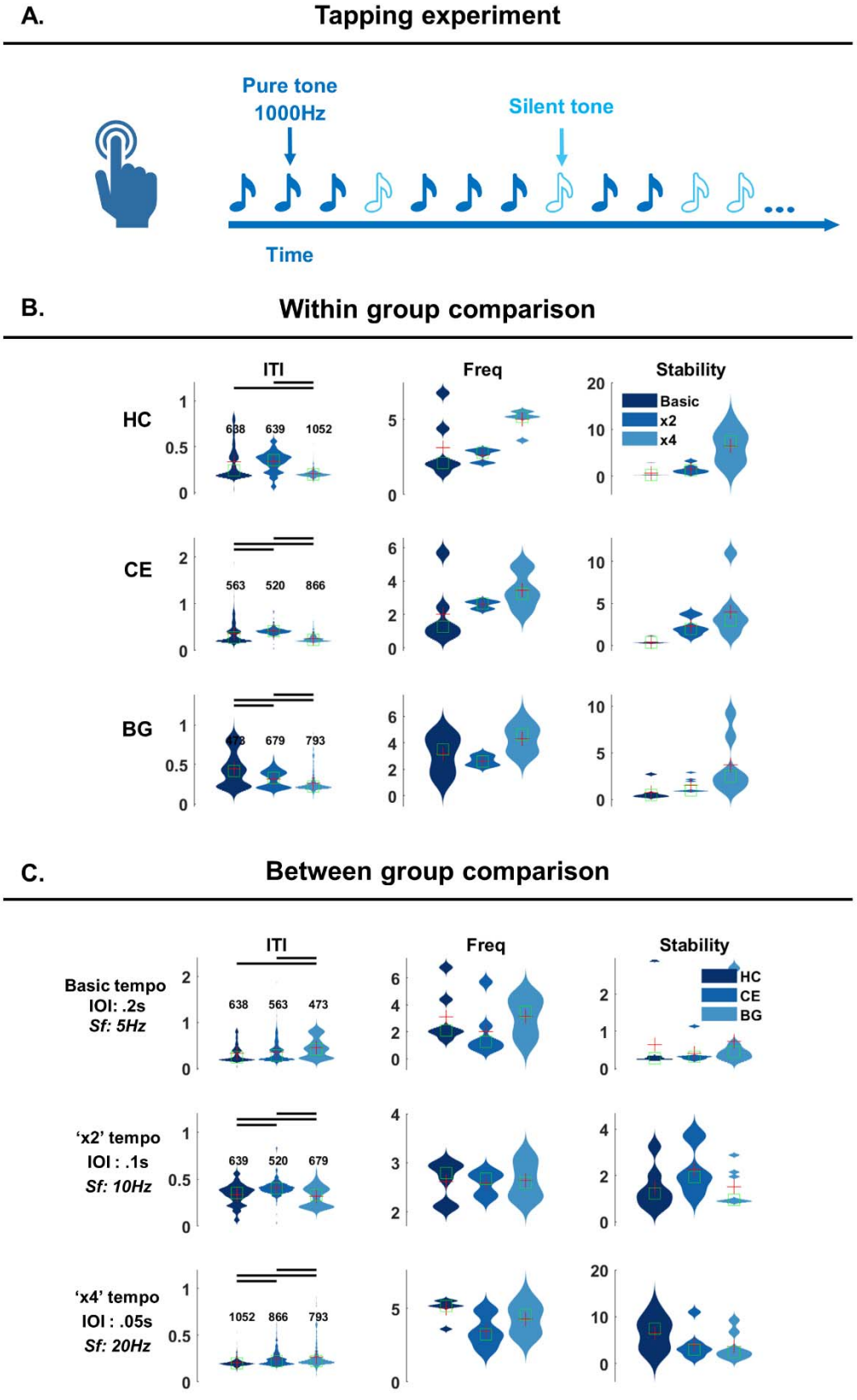

Figure 4 – Tapping experiment and group comparisons.

A: experimental design: participants listened to auditory sequences at three different speeds and were asked to synchronize their tapping to the perceived beat, while keeping the tapping at a comfortable rate. These sequences included pure tones at 1000Hz and silent tones. The inter-onset-intervals (IOIs) varied from the basic tempo (IOI: .2s) to the 'x2' tempo (IOI: .1s) and 'x4' tempo (IOI: .05s), resulting in stimulation frequencies (Sf) of 5, 10 and 20 Hz respectively. B: Within group comparisons statistically assessed the difference in inter-tap-intervals (ITI) per group (each row), and across speeds (the three distributions per plot). Thick, black, horizontal lines report significant differences across tempi, per group. Next to ITI, we also estimated the tapping frequency (Freq) and tapping stability (in order). C: Between group comparisons statistically assessed the difference in ITI across groups (the three distributions per plot), per tempo. Thick, black, horizontal lines report significant differences across groups, per tempo. Next to ITI, we also estimated the tapping frequency (Freq) and tapping stability (in order).

3.3. Link between Tapping - EEG

Further analyses assessed the link between Tapping Entropy (Tap E; light blue) and Tapping Stability (Tap S; dark blue) with the metrics derived from the individual's EEG data analyses (Fig. 5). Given the low number of participants per group, these correlations present exploratory analyses, and no conclusions are drawn on these observations. The correlation strength (rho values) is represented in Fig. 5 with the thickness of the line connecting each node. Rho values below .5 were masked out. Positive and negative rho values are also provided in Suppl. Tab. 18.

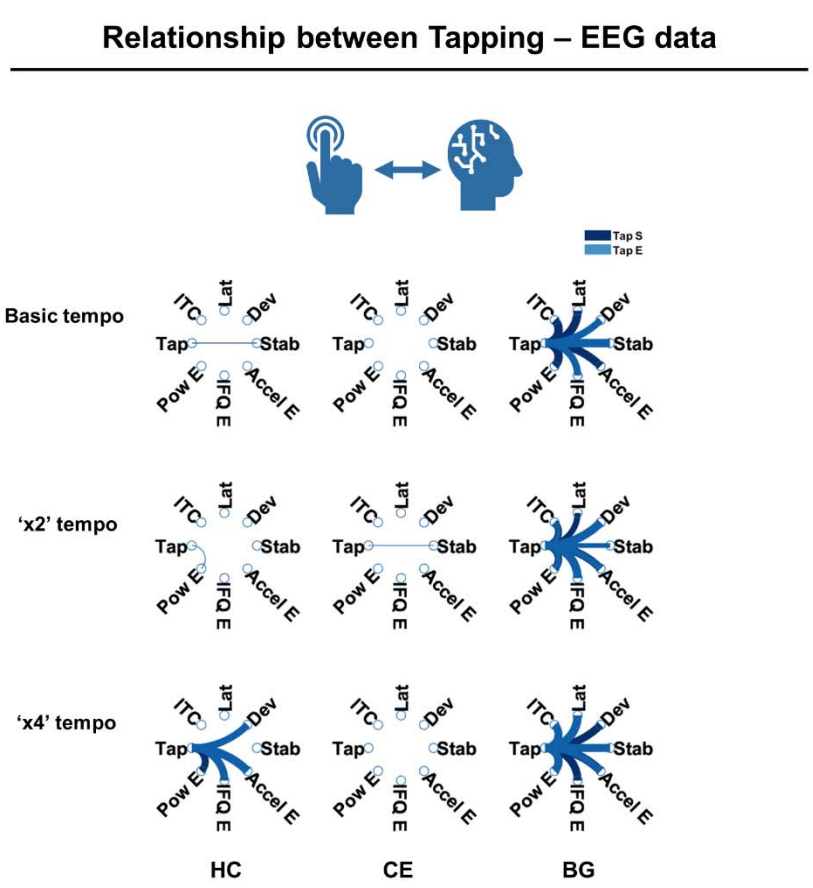

Figure 5 – Relationship between Tapping and EEG data.

Exploratory analyses assessed the link between tapping metrics of stability (Tap S; dark blue) and Shannon entropy (Tap E; light blue) with EEG-derived metrics of Inter-trial-coherence (ITC), power entropy (Pow E), entropy in instantaneous frequency (IFQ E), acceleration entropy (Accel E), Acceleration Stability (Stab), Deviation (Dev) and Latency (Lat). Correlations were performed independently per groups (organized column-wise) and tapping speeds (organized in rows).

4. Discussion

We investigated the causal contributions of the cerebellum (CE) and the basal ganglia (BG) to sensory and sensorimotor processes underlying the detection, production and synchronization ('DPS') with basic auditory rhythms. Using EEG, we assessed the neural dynamics of temporal processing, unravelling group differences in *when*, *if*, and *how* healthy controls (HC), CE, and BG lesion patients process temporal regularities. Next, a behavioral experiment probed their capacity for DPS when tapping to temporally regular acoustic sequences at different rates.

Starting from the behavioral experiment, we found significant group differences across tapping

rates. CE patients showed similar tapping rates as HCs for the basic rate and more stable tapping than the other groups for the 'x2' rate, where they tapped faster. However, the tapping at 'x4' was slower and more variable than for the other two groups, and their stability was lower than that of the HCs. Analyses of delta-band neural dynamics revealed that CE patients' delta power and instantaneous frequency were comparable to the HCs. However, they showed lower stability and reduced phase coherence, confirming preserved yet deteriorated sensitivity to temporal regularity in the acoustic sequences. These observations are in line with previous evidence, where CE patients showed intact sensitivity to the temporal structure of auditory sequences (Schwartze & Kotz, 2021), but heterogenous encoding of the precise timing of event onsets (Grube, Cooper, et al., 2010b; Nozaradan et al., 2017), ultimately affecting the production of and synchronization with rhythms especially at faster rates (Ivry & Keele, 1989; Ivry, Keele & Diener, 1988; Schwartze et al., 2016).

Compared to HCs and CE patients, BG patients' tapping frequency did not follow the increase in tempo rates but followed a U-shape. Large inter-individual variability was present especially at the basic tempo, with some patients tapping very fast while others tapped more regularly. BG patients' tapping stability was lower than that of the other groups in the fastest tempo. In line with these observations, EEG results for delta-band neural activity revealed stronger power variations, reduced instantaneous frequency, stability, and phase coherence in BG patients when listening to isochronous auditory sequences. We consider that altered sensory encoding of temporal regularity might have influenced the patients' capacity to produce and synchronize efficiently with an external rhythm. These findings are in line with previous results showing altered processing of salient periodicities in BG patients (Nozaradan et al., 2017) even in simple auditory sequences (Schwartze et al., 2015), and confirm that the heterogeneity in tapping behavior and difficulties in adapting to tempo changes are related to BG dysfunctions (Schwartze et al., 2011b).

Although exploratory, correlation analyses further revealed a link between tapping behavior (entropy and stability) and brain-derived metrics of dynamics (e.g., power entropy, acceleration, stability), specifically for the BG patients. However, given the small sample size and low statistical power, we refrain from any speculative interpretations of these preliminary results.

The newly employed methods allowed characterizing the role of delta-band oscillations in basic rhythm processing: we showed that delta oscillations fluctuate over time, *tuning in* and *out of*

perceived acoustic regularity in auditory sequences by dynamically accelerating and slowing down from silence to listening periods. These observations support the *dynamic attending* hypothesis (Jones & Boltz, 1989; Large & Jones, 1999), and confirm the role of low-frequency oscillations (Schroeder & Lakatos, 2009) in detecting, producing, and synchronizing with temporal regularities in an auditory environment. On the other hand, the current approach also confirmed the fundamental role of the BG and CE in an extended cortico-subcortical-cortical network underlying rhythm and timing processing (Criscuolo, Pando-Naude, et al., 2022; Kasdan et al., 2022; Kotz et al., 2018; Schwartze & Kotz, 2013). In fact, we showed that while the healthy brain could flexibly and dynamically respond to and synchronize with sensory inputs, patients with lesions in the BG and CE did not. Patients showed a degree of heterogeneity and deteriorated capacity to synchronize ongoing neural activity to temporal regularities in the acoustic environment, which ultimately resulted in altered capacity to produce stable tapping and to synchronize behavior with external rhythms. Differently from our hypotheses, however, we could not clearly dissociate CE from BG timing functions. We argue that our experimental setup and/or the adopted analytical approach may have played a role. For instance, use of isochronous auditory sequences as opposed to complex auditory rhythms may represent the first limitation, as these stimuli may have been suboptimal to dissociate CE-related sensory timing computations from BG-related temporal predictions. Secondly, differently from the typical tone-locked analysis approach, we here investigated the neural dynamics of rhythm tracking at the sequence-level. This choice allowed us to characterize the frequency, acceleration, and stability of neural waves tuning towards auditory rhythms. However, such approach does not provide an indication of inter-individual variability in the amplitude and latency of event-related responses to each tone onset along the sequence. Third, we have previously discussed that BG and CE are part of a widespread cortico-subcortical network engaging in rhythm processing. Thus, a lesion in these subcortical regions may not necessarily impact basic rhythm processing. In fact, we know from the animal literature that there are neurons in the cortex acting as ‘neural chronometer’ encoding the passage of time and the precise timing of sensory events (Merchant et al., 2011; Merchant, Harrington, et al., 2013; Merchant, Pérez, et al., 2013). These cortical neurons may take over timing computations as a functional reorganization mechanism after subcortical brain lesions, ultimately preventing to characterize the link between focal subcortical lesion and impaired timing functions. Finally, another limitation lies in the difficulty to distinguish fine-grained

timing processing in absence of spatio-temporally resolved data. In this perspective, this research field would benefit from a more accurate characterization of the time-course, strength and directionality of information flow during rhythm processing. Such approach would allow to monitor the interplay and the causal relationship between cortico-subcortical regions, as well as between the BG and CE. Furthermore, it would enable to characterize the frequency-specificity and directionality of influence of some timing computations. Existing literature suggests delta-, as well as beta-band activity to be prominent in subcortical and cortical brain regions (Bartolo et al., 2014; Bartolo & Merchant, 2015; Keitel et al., 2017; Keitel & Gross, 2016) and to be linked to predictive priming of sensory regions (Arnal, 2012; Engel & Fries, 2010). In other words, the anticipatory alignment of beta-band activity to the *when* of salient events (Fujioka et al., 2012, 2015) couples with bottom-up delta-band activity (Abbasi et al., 2018; Arnal et al., 2015; Merchant et al., 2015; Saleh et al., 2010) to instantiate motor-to-auditory predictions in support of adaptive behavior. Thus, our focus on scalp activity and on delta-band activity only prevents a full characterization of bottom-up and top-down mechanisms of temporal processing and prediction. Altogether, we encourage future studies to complement the current findings with investigations of beta-band activity, with a particular focus on event-related dynamics and beta-delta functional coupling. Such a complementary approach would deepen our understanding of the neurophysiological mechanisms underlying intra- and inter-individual variabilities in the capacities to detect, produce and synchronize with temporal regularities in the sensory environment, and to ultimately produce adaptive behavior.

5. Conclusions

The capacities to encode the precise timing of the sensory events around us, and to time our (re-)actions to changes in the environment are pivotal to act and adapt in a dynamically changing environment. In this study, we explored the rich and variegated landscape of neural oscillatory dynamics, and assessed *if*, *when* and *how* neural oscillations processed the temporal regularity in acoustic sequences. BG and CE lesions impacted the neurophysiological encoding of the rhythm and further affected the ability to produce and synchronize behavior (tapping) to external stimuli.

Author contributions

S.A.K., M.S., C.O., S.N., conceptualized both or one part of the study.

S.A.K., M.S., C.O., collected the data.

A.C. designed and performed data analyses.

A.C., S.A.K., M.S., S.N., interpreted the results and wrote the manuscript.

Declaration of Competing Interest

The authors declare no competing interests.

Acknowledgments

The authors would like to thank Anne-Kathrin Franz, Christian Obermeier and Heike Boethel for support during data acquisition, Anika Stockert for support in the preparation of the clinical data and Julio Rodriguez-Larios for initial data discussion and analysis exploration.

References

Abbasi, O., Hirschmann, J., Storzer, L., Özkurt, T. E., Elben, S., Vesper, J., Wojtecki, L., Schmitz, G., Schnitzler, A., & Butz, M. (2018). Unilateral deep brain stimulation suppresses alpha and beta oscillations in sensorimotor cortices. *NeuroImage*. https://doi.org/10.1016/j.neuroimage.2018.03.026

Arnal, L. H. (2012). Predicting "When" Using the Motor System's Beta-Band Oscillations. *Frontiers in Human Neuroscience*, *6*. https://doi.org/10.3389/fnhum.2012.00225

Arnal, L. H., Doelling, K. B., & Poeppel, D. (2015). Delta-beta coupled oscillations underlie temporal prediction accuracy. *Cerebral Cortex*, *25*(9), 3077–3085. https://doi.org/10.1093/cercor/bhu103

Arnal, L. H., & Giraud, A. L. (2012). Cortical oscillations and sensory predictions. In *Trends in Cognitive Sciences* (Vol. 16, Issue 7, pp. 390–398). https://doi.org/10.1016/j.tics.2012.05.003

Bartolo, R., & Merchant, H. (2015). β oscillations are linked to the initiation of sensory-cued movement sequences and the internal guidance of regular tapping in the monkey. *Journal of Neuroscience*. https://doi.org/10.1523/JNEUROSCI.4570-14.2015

Bartolo, R., Prado, L., & Merchant, H. (2014). Information Processing in the Primate Basal Ganglia during Sensory-Guided and Internally Driven Rhythmic Tapping. *Journal of Neuroscience*, *34*(11), 3910–3923. https://doi.org/10.1523/JNEUROSCI.2679-13.2014

Cohen, M. X. (2014). Analyzing Neural Time Series Data: Theory and Practice. In *MIT Press*. https://doi.org/10.1017/CBO9781107415324.004

Cravo, A. M., Rohenkohl, G., Wyart, V., & Nobre, A. C. (2013). Temporal expectation enhances contrast sensitivity by phase entrainment of low-frequency oscillations in visual cortex. *Journal of Neuroscience*, *33*(9), 4002–4010. https://doi.org/10.1523/JNEUROSCI.4675-12.2013

Criscuolo, A, Schwartze, M., Henry, M. J., Obermeier, C., & Kotz, S. A. (2023). Individual neurophysiological signatures of spontaneous rhythm processing. *NeuroImage*, *273*, 120090. https://doi.org/10.1016/j.neuroimage.2023.120090

Criscuolo, Antonio, Pando-Naude, V., Bonetti, L., Vuust, P., & Brattico, E. (2022). An ALE meta-analytic review of musical expertise. *Scientific Reports* |, *12*. https://doi.org/10.1038/s41598-022-14959-4

Criscuolo, Antonio, Schwartze, M., & Kotz, S. A. (2022). Cognition through the lens of a body–brain dynamic system. *Trends in Neurosciences*. https://doi.org/10.1016/J.TINS.2022.06.004

Criscuolo, Antonio, Schwartze, M., Prado, L., Ayala, Y., Merchant, H., & Kotz, S. A. (2023). Macaque monkeys and humans sample temporal regularities in the acoustic environment. *Progress in Neurobiology*, *229*, 102502. https://doi.org/10.1016/J.PNEUROBIO.2023.102502

Engel, A. K., & Fries, P. (2010). Beta-band oscillations-signalling the status quo? In *Current Opinion in Neurobiology*. https://doi.org/10.1016/j.conb.2010.02.015

Friston, K. (2005). A theory of cortical responses. *Philosophical Transactions of the Royal Society B: Biological Sciences*. https://doi.org/10.1098/rstb.2005.1622

Fujioka, T., Ross, B., & Trainor, L. J. (2015). Beta-band oscillations represent auditory beat and its metrical hierarchy in perception and imagery. *Journal of Neuroscience*. https://doi.org/10.1523/JNEUROSCI.2397-15.2015

Fujioka, T., Trainor, L. J., Large, E. W., & Ross, B. (2009). Beta and gamma rhythms in human auditory cortex during musical beat processing. *Annals of the New York Academy of Sciences*. https://doi.org/10.1111/j.1749-6632.2009.04779.x

Fujioka, T., Trainor, L. J., Large, E. W., & Ross, B. (2012). Internalized Timing of Isochronous Sounds Is Represented in Neuromagnetic Beta Oscillations. *Journal of Neuroscience*, *32*(5), 1791–1802. https://doi.org/10.1523/JNEUROSCI.4107-11.2012

Gámez, J., Yc, K., Ayala, Y. A., Dotov, D., Prado, L., & Merchant, H. (2018). Predictive rhythmic tapping to isochronous and tempo changing metronomes in the nonhuman primate. *Annals of the New York Academy of Sciences*. https://doi.org/10.1111/nyas.13671

Grahn, J. A. (2009). The Role of the Basal Ganglia in Beat Perception. *Annals of the New York Academy of Sciences*, *1169*(1), 35–45. https://doi.org/10.1111/j.1749-6632.2009.04553.x

Grahn, J. A., & Brett, M. (2009a). Impairment of beat-based rhythm discrimination in Parkinson's disease. *Cortex*, *45*(1), 54–61. https://doi.org/10.1016/j.cortex.2008.01.005

Grahn, J. A., & Brett, M. (2009b). Impairment of beat-based rhythm discrimination in Parkinson's disease. *Cortex*, *45*(1), 54–61. https://doi.org/10.1016/J.CORTEX.2008.01.005

Greenfield, M. D., Aihara, I., Amichay, G., Anichini, M., & Nityananda, V. (2021). Rhythm interaction in animal groups: selective attention in communication networks. *Philosophical*

Transactions of the Royal Society B, *376*(1835). https://doi.org/10.1098/RSTB.2020.0338

Greenfield, M. D., Honing, H., Kotz, S. A., & Ravignani, A. (2021). Synchrony and rhythm interaction: From the brain to behavioural ecology. *Philosophical Transactions of the Royal Society B: Biological Sciences*, *376*(1835). https://doi.org/10.1098/rstb.2020.0324

Grube, M., Cooper, F. E., Chinnery, P. F., & Griffiths, T. D. (2010a). Dissociation of duration-based and beat-based auditory timing in cerebellar degeneration. *Proceedings of the National Academy of Sciences of the United States of America*. https://doi.org/10.1073/pnas.0910473107

Grube, M., Cooper, F. E., Chinnery, P. F., & Griffiths, T. D. (2010b). Dissociation of duration-based and beat-based auditory timing in cerebellar degeneration. *Proceedings of the National Academy of Sciences of the United States of America*, *107*(25), 11597–11601. https://doi.org/10.1073/PNAS.0910473107/SUPPL_FILE/PNAS.200910473SI.PDF

Grube, M., Lee, K. H., Griffiths, T. D., Barker, A. T., & Woodruff, P. W. (2010). Transcranial magnetic theta-burst stimulation of the human cerebellum distinguishes absolute, duration-based from relative, beat-based perception of subsecond time intervals. *Frontiers in Psychology*. https://doi.org/10.3389/fpsyg.2010.00171

Ivry, R. B., & Keele, S. W. (1989). Timing Functions of The Cerebellum. *Journal of Cognitive Neuroscience*, *1*(2), 136–152. https://doi.org/10.1162/JOCN.1989.1.2.136

Ivry, R. B., Keele, S. W., & Diener, H. C. (1988). Dissociation of the lateral and medial cerebellum in movement timing and movement execution. *Volume 73, Issue 1, Pages 167 - 180*, *73*(1), 167–180. https://doi.org/10.1007/BF00279670

Ivry, Richard B., & Schlerf, J. E. (2008). Dedicated and intrinsic models of time perception. *Trends in Cognitive Sciences*, *12*(7), 273–280. https://doi.org/10.1016/J.TICS.2008.04.002

Jones, M. R., & Boltz, M. (1989). Dynamic Attending and Responses to Time. *Psychological Review*, *96*(3), 459–491. https://doi.org/10.1037/0033-295X.96.3.459

Kasdan, A. V., Burgess, A. N., Pizzagalli, F., Scartozzi, A., Chern, A., Kotz, S. A., Wilson, S. M., & Gordon, R. L. (2022). Identifying a brain network for musical rhythm: A functional neuroimaging meta-analysis and systematic review. *Neuroscience & Biobehavioral Reviews*, *136*, 104588. https://doi.org/10.1016/J.NEUBIOREV.2022.104588

Keitel, A., & Gross, J. (2016). Individual Human Brain Areas Can Be Identified from Their Characteristic Spectral Activation Fingerprints. *PLoS Biology*, *14*(6), 1–22.

https://doi.org/10.1371/journal.pbio.1002498

Keitel, A., Ince, R. A. A., Gross, J., & Kayser, C. (2017). NeuroImage Auditory cortical delta-entrainment interacts with oscillatory power in multiple fronto-parietal networks. *NeuroImage*, *147*(November 2016), 32–42. https://doi.org/10.1016/j.neuroimage.2016.11.062

Knolle, F., Schröger, E., Baess, P., & Kotz, S. A. (2012). The cerebellum generates motor-to-auditory predictions: ERP lesion evidence. *Journal of Cognitive Neuroscience*, *24*(3), 698–706. https://doi.org/10.1162/jocn_a_00167

Knolle, F., Schröger, E., & Kotz, S. A. (2013). Cerebellar contribution to the prediction of self-initiated sounds. *Cortex*, *49*(9), 2449–2461. https://doi.org/10.1016/j.cortex.2012.12.012

Kotz, S. A., Ravignani, A., & Fitch, W. T. (2018). The Evolution of Rhythm Processing. *Trends in Cognitive Sciences*, *22*(10), 896–910. https://doi.org/10.1016/j.tics.2018.08.002

Kotz, Sonja A., & Schmidt-Kassow, M. (2015). Basal ganglia contribution to rule expectancy and temporal predictability in speech. *Cortex*. https://doi.org/10.1016/j.cortex.2015.02.021

Lakatos, P., Karmos, G., Mehta, A. D., Ulbert, I., & Schroeder, C. E. (2008). Entrainment of neuronal oscillations as a mechanism of attentional selection. *Science*, *320*(5872), 110–113. https://doi.org/10.1126/science.1154735

Lakatos, P., Musacchia, G., O'Connel, M. N., Falchier, A. Y., Javitt, D. C., & Schroeder, C. E. (2013). The Spectrotemporal Filter Mechanism of Auditory Selective Attention. *Neuron*, *77*(4), 750–761. https://doi.org/10.1016/j.neuron.2012.11.034

Lakatos, P., Shah, A. S., Knuth, K. H., Ulbert, I., Karmos, G., & Schroeder, C. E. (2005). An Oscillatory Hierarchy Controlling Neuronal Excitability and Stimulus Processing in the Auditory Cortex An Oscillatory Hierarchy Controlling Neuronal Excitability and Stimulus Processing in the Auditory Cortex. *Journal of Neurophysiology*, *94*, 1904–1911. https://doi.org/10.1152/jn.00263.2005

Large, E. W., & Jones, M. R. (1999). The dynamics of attending: How people track time-varying events. *Psychological Review*, *106*(1), 119–159. https://doi.org/10.1037/0033-295X.106.1.119

Merchant, H., Grahn, J., Trainor, L., Rohrmeier, M., & Fitch, W. T. (2015). Finding the beat: A neural perspective across humans and non-human primates. *Philosophical Transactions of the Royal Society B: Biological Sciences*. https://doi.org/10.1098/rstb.2014.0093

Merchant, H., Harrington, D. L., & Meck, W. H. (2013). Neural Basis of the Perception and Estimation of Time. *Annual Review of Neuroscience*. https://doi.org/10.1146/annurev-neuro-062012-170349

Merchant, H., Pérez, O., Zarco, W., & Gámez, J. (2013). Interval tuning in the primate medial premotor cortex as a general timing mechanism. *Journal of Neuroscience*. https://doi.org/10.1523/JNEUROSCI.5513-12.2013

Merchant, H., Zarco, W., Pérez, O., Prado, L., & Bartolo, R. (2011). Measuring time with different neural chronometers during a synchronization-continuation task. *Proceedings of the National Academy of Sciences of the United States of America*. https://doi.org/10.1073/pnas.1112933108

Morillon, B., Schroeder, C. E., Wyart, V., & Arnal, L. H. (2016). Temporal prediction in lieu of periodic stimulation. *Journal of Neuroscience*. https://doi.org/10.1523/JNEUROSCI.0836-15.2016

Nobre, A. C., Rohenkohl, G., & Stokes, M. (2012). Nervous Anticipation : Top-Down Biasing across Space and Time. *Cognitive Neuroscience of Attention*.

Nozaradan, S., Schwartze, M., Obermeier, C., & Kotz, S. A. (2017). Specific contributions of basal ganglia and cerebellum to the neural tracking of rhythm. *Cortex*, *95*, 156–168. https://doi.org/10.1016/j.cortex.2017.08.015

Oostenveld, R., Fries, P., Maris, E., & Schoffelen, J. M. (2011). FieldTrip: Open source software for advanced analysis of MEG, EEG, and invasive electrophysiological data. *Computational Intelligence and Neuroscience*. https://doi.org/10.1155/2011/156869

Ross, J., Iversen, J., & Balasubramaniam, R. (2018). Dorsal Premotor Contributions to Auditory Rhythm Perception: Causal Transcranial Magnetic Stimulation Studies of Interval, Tempo, and Phase. In *bioRxiv*. https://doi.org/10.1101/368597

Saleh, M., Reimer, J., Penn, R., Ojakangas, C. L., & Hatsopoulos, N. G. (2010). Fast and Slow Oscillations in Human Primary Motor Cortex Predict Oncoming Behaviorally Relevant Cues. *Neuron*. https://doi.org/10.1016/j.neuron.2010.02.001

Schroeder, C. E., & Lakatos, P. (2009). Low-frequency neuronal oscillations as instruments of sensory selection. *Trends in Neurosciences*, *32*(1), 9–18. https://doi.org/10.1016/j.tins.2008.09.012

Schwartze, M., Keller, P. E., & Kotz, S. A. (2016a). Spontaneous, synchronized, and corrective

timing behavior in cerebellar lesion patients. *Behavioural Brain Research*, *312*, 285–293. https://doi.org/10.1016/j.bbr.2016.06.040

Schwartze, M., Keller, P. E., & Kotz, S. A. (2016b). Spontaneous, synchronized, and corrective timing behavior in cerebellar lesion patients. *Behavioural Brain Research*, *312*, 285–293. https://doi.org/10.1016/J.BBR.2016.06.040

Schwartze, M., Keller, P. E., Patel, A. D., & Kotz, S. A. (2011a). The impact of basal ganglia lesions on sensorimotor synchronization, spontaneous motor tempo, and the detection of tempo changes. *Behavioural Brain Research*, *216*(2), 685–691. https://doi.org/10.1016/j.bbr.2010.09.015

Schwartze, M., Keller, P. E., Patel, A. D., & Kotz, S. A. (2011b). The impact of basal ganglia lesions on sensorimotor synchronization, spontaneous motor tempo, and the detection of tempo changes. *Behavioural Brain Research*, *216*(2), 685–691. https://doi.org/10.1016/J.BBR.2010.09.015

Schwartze, M., & Kotz, S. A. (2013). A dual-pathway neural architecture for specific temporal prediction. *Neuroscience and Biobehavioral Reviews*, *37*(10), 2587–2596. https://doi.org/10.1016/j.neubiorev.2013.08.005

Schwartze, M., & Kotz, S. A. (2021). Delayed auditory encoding and variable representation of stimulus regularity in cerebellar lesion patients. *BioRxiv*, 2021.02.06.430035. https://doi.org/10.1101/2021.02.06.430035

Schwartze, M., Stockert, A., & Kotz, S. A. (2015). Striatal contributions to sensory timing: Voxel-based lesion mapping of electrophysiological markers. *Cortex*, *71*, 332–340. https://doi.org/10.1016/j.cortex.2015.07.016

Snyder, J. S., & Large, E. W. (2005). Gamma-band activity reflects the metric structure of rhythmic tone sequences. *Cognitive Brain Research*, *24*(1), 117–126. https://doi.org/10.1016/j.cogbrainres.2004.12.014

Teki, S., Grube, M., & Griffiths, T. D. (2011). A unified model of time perception accounts for duration-based and beat-based timing. *Frontiers in Integrative Neuroscience*, *5*(DECEMBER), 20319. https://doi.org/10.3389/FNINT.2011.00090/BIBTEX

Teki, S., Grube, M., Kumar, S., & Griffiths, T. D. (2011). Distinct neural substrates of duration-based and beat-based auditory timing. *Volume 31, Issue 10, Pages 3805 - 3812*, *31*(10), 3805–3812. https://doi.org/10.1523/JNEUROSCI.5561-10.2011